Available online at www.sciencedirect.com
SCIENCE DIRECT®
Molecular Brain Research 121 (2004) 37–49
MOLECULAR BRAIN RESEARCH
www.elsevier.com/locate/molbrainres

Research report

Increased expression of AMPA receptor subunits in the nucleus of the solitary tract in the spontaneously hypertensive rat

Sikha Saha*, Emma J. Spary, Azhar Maqbool, Aruna Asipu, Eric K.A. Corbett, Trevor F.C. Batten

School of Medicine, University of Leeds, Leeds LS2 9JT, UK

Accepted 13 November 2003

Abstract

The expression of α-amino-3-hydroxy-5-methylisoxazole-4-propionic acid (AMPA) receptor subunits GluR1–4 in the nucleus of the solitary tract (NTS) of adult Wistar rats was examined by polymerase chain reaction (PCR), and the neuronal localisation of these receptor subunits in the NTS were confirmed by immunohistochemistry using subunit-specific antibodies. Semi-quantitative PCR was used to investigate differences in AMPA receptor subunit expression between spontaneously hypertensive rats (SH) and age-matched normotensive Wistar Kyoto rats (WKY). All four receptor subunits were expressed in both strains, but compared to WKY, total AMPA receptor and the GluR3 mRNA expressions were significantly higher in SH. No differences were detected in cDNA form the cerebral cortex or cerebellum. Immunolabelling for GluRs 1, 2 and 2/3 in the neuropil relative to neuronal somata in the cardioregulatory areas of the NTS appeared to be increased in SH, with an overall increase in the density of GluR2/3 labelling in the medial and commissural NTS of SH. These results indicate a possible role for changes in AMPA receptor subunit expression in NTS neurones, involving an increase in GluR3 associated with development of hypertension in SH.

Theme: Endocrine and automatic regulation
Topic: Cardiovascular regulation

Keywords: Glutamate receptor; Nucleus of the solitary tract; Hypertension; Polymerase chain reaction; Immunohistochemistry

1. Introduction

The functions of the excitatory amino acid glutamate in the central nervous system (CNS) are mediated through activation of both ligand-gated ionotropic receptors and G-protein-coupled metabotropic receptors. On the basis of agonist affinities, ionotropic receptors are classified into three subtypes: α-amino-3-hydroxy-5-methylisoxazole-4-propionic acid (AMPA), *N*-methyl-D-aspartic acid (NMDA), and kainate receptors [28]. AMPA receptors are the principal mediators of fast excitatory neurotransmission and are abundant throughout the CNS [7]. Molecular cloning of cDNAs identified four closely related subunits, designated GluR1 to GluR4 for the rat, or GluR-A to GluR-D for the mouse [7,17,43]. Each cloned AMPA subunit was found to occur in two alternately spliced ''flip and flop'' isoforms, which are differentially expressed throughout the brain [44].

Evidence has suggested that functional AMPA receptors exist as pentameric complexes [7] or more probably tetrameric complexes [24] made up of heterologous subunits and single cell analysis demonstrated that Purkinje cells can express up to five different AMPA subunits or splice variants [21]. The expression of individual AMPA subunits changes during normal development, and may also underlie neuroplastic processes such as long-term potentiation and long-term depression, and certain neurological diseases [7,31]. In particular, expression of certain edited GluR2 transcripts confers low Ca^{2+} permeability [7]. It thus seems reasonable to propose that chronic hypertension may be accompanied by a change in AMPA subunit expression in areas of the CNS that regulate blood pressure.

The nucleus of the solitary tract (NTS) is the primary medullary region for co-ordination and integration of sen-

* Corresponding author. Institute for Cardiovascular Research, Worsley Building, University of Leeds, Leeds LS2 9JT, UK. Tel.: +44-113-343-4172; fax: +44-113-343-4803.
E-mail address: cvsss@leeds.ac.uk (S. Saha).

0169-328X/$ - see front matter © 2003 Elsevier B.V. All rights reserved.
doi:10.1016/j.molbrainres.2003.11.003

sory afferent inputs derived from the cardiovascular, respiratory, gastrointestinal and gustatory systems [23,45]. Neurophysiological and pharmacological evidence points to a role for glutamate, acting predominantly at non-NMDA receptors, in cardiovascular regulatory mechanisms in the NTS [4,22,49]. The distribution of AMPA receptor subunit immunoreactivities in the dorsal vagal complex has recently been described for the rat [18] and the cat [3], and the GluR1 and GluR2 subunits have been detected on rat NTS neurones that are activated by baroreceptor inputs [56]. There is evidence that during the development of hypertension in rats the glutamatergic systems are affected at several points in the reflex pathways of the medulla including the NTS, although there are some inconsistencies in the results. For example, the number of glutamatergic NTS neurones providing output to the ventrolateral medulla is reduced in the spontaneously hypertensive (SH) rat compared to age-matched normotensive Wistar–Kyoto (WKY) rats [48]. The incidence of dendrites and spines in the NTS displaying GluR1 immunoreactivity is increased in SH compared to WKY [1], suggesting that postsynaptic glutamate receptor subunits in the NTS may be altered by chronic elevations in arterial pressure. No such differences in total AMPA receptor binding sites between SH and control rats were found by receptor autoradiography [6]. However, accurate quantitation of differences in receptor labelling in anatomically and functionally heterogeneous brain areas like the NTS is difficult using autoradiography and immunohistochemistry.

Here, we have employed semi-quantitative reverse transcription polymerase chain reaction (RT-PCR) to determine whether mRNA expression of both total and individual AMPA receptor subunits in the NTS of the adult SH rat is different from that seen in normotensive WKY rats. Then, using specific antibodies we have investigated differences in the tissue labelling patterns for the individual GluR1–4 receptor subunits between the two strains, which might be related to the pathogenesis of hypertension.

2. Materials and methods

2.1. Tissue preparation

Adult male Wistar rats (160–220 g, $n=6$) were supplied by the University of Leeds Central Biomedical Services. Twelve-week-old male SH and age-matched WKY rats (200–250 g, $n=6$ of each) were supplied by Charles River Margate, Kent, UK. All experimental rats were killed by decapitation under halothane (5% in O_2) anaesthesia in accordance with the regulations of the UK Animals (Scientific Procedures) Act, 1986. Brains were dissected out and rapidly frozen on dry ice. Coronal slices of 0.5–1 mm thickness were cut from the brainstem and tissue punches were collected from the medial NTS with a 0.69 mm corer under a ×5 dissecting microscope. The placement of the tissue punches in the slices was verified (Fig. 1) after brief fixation (~ 1h) in phosphate buffered 4% paraformaldehyde, resectioning at 50 μm thickness on a vibrating microtome and histological staining with cresyl fast violet. As a positive control, tissue was also dissected from the cerebellum and cerebral cortex.

2.2. Reverse transcription polymerase chain reaction

Total RNA was isolated and reverse-transcribed to first-strand cDNA as described previously [36]. PCR was performed in a 25-μl reaction containing 2 μl cDNA, Taq DNA polymerase reaction buffer (50mM Tris–HCl, pH 8.5, 1.5 mM $MgCl_2$), 200 μM each dNTP and 1.5 U Taq DNA polymerase in a Perkin Elmer GeneAmp 9700 (Applied Biosystems), with 0.8 μM subunit-specific primers (Table 1) designed using GeneFisher (http://bibiserv.techfak.uni-bielefeld.de/genefisher). Amplification was initiated by a 5-min pre-incubation at 95 °C, followed by 35 cycles of 95 °C for 30 s, 60 °C for 30 s and 72 °C for 1 min, with a 7-min extension step at 72 °C. Negative controls included amplification of RNA without reverse transcription and water. Products were separated by electrophoresis on agarose gels containing ethidium bromide and visualised under UV light.

2.3. Specificity test for PCR product by endonuclease digestion and sequencing

The veracity of PCR amplicons was established by restriction analysis with specific endonuclease enzymes (Fig. 3) as previously reported [36], and by BigDye terminator cycle sequencing in an ABI PRISM 377 DNA sequencer with analysis software version 3.3.

2.4. Semi-quantitative analysis of RT-PCR products in SH and WKY rats

Semi-quantitative PCR was based on co-amplification of the target cDNA with primer pairs (Table 1) for the AMPA subunit (1.2 μM) and the "housekeeping gene" glyceraldehyde-3-phosphate dehydrogenase (GAPDH, 0.2 μM) for 30 cycles, in a single tube in order to avoid tube-to-tube variations. Pilot studies determined optimal primer concen-

Fig. 1. Micrographs showing the placement of unilateral or bilateral tissue punches in the dorsomedial medulla oblongata, in unstained ~ 0.5 mm sections (A and B) and 50 μm sections stained with cresyl fast violet (C and D). Note that the area of tissue removed is mainly from the NTS subnuclei medial to the tractus solitarius (ts), i.e. medial (me) and dorsomedial (dm) subnuclei, but may also include some tissue from the gracile nucleus (Gr) and dorsal vagal nucleus (DVN). The approximate level of sectioning in mm relative to bregma [30] is shown bottom left of each panel. Additional abbreviations: 4v, 4th ventricle; AP, area postrema; com, commissural subnucleus; Cu, cuneate nucleus; gel, gelatinosus subnucleus; Gr, gracile nucleus; sp, sub-postremal subnucleus; vl, ventrolateral subnucleus; XII, hypoglossal motor nucleus. Scale bars = 0.5 mm.

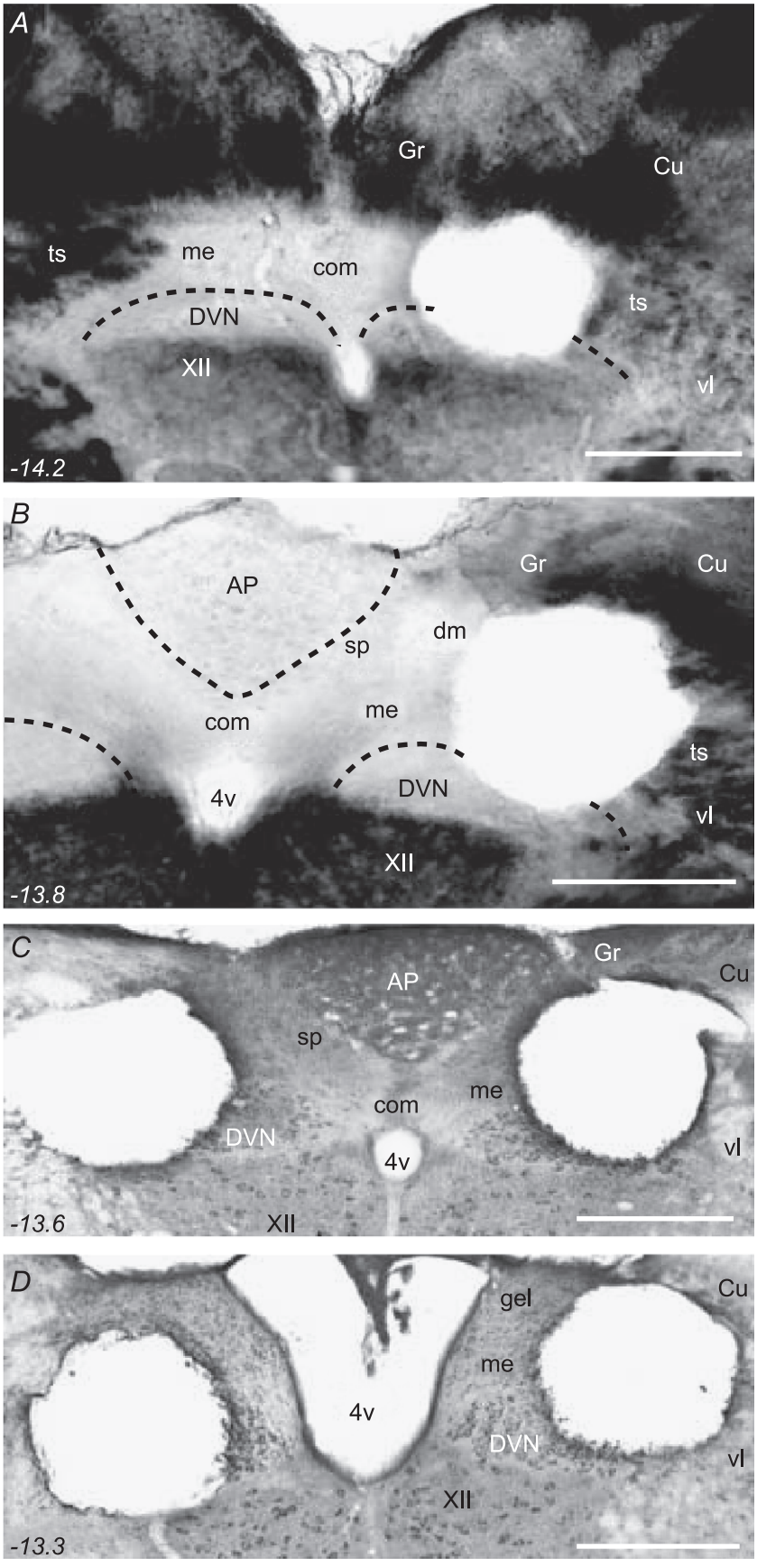
A
Gr
Cu
ts
me
com
DVN
XII
ts
vl
-14.2
B
AP
Gr
Cu
dm
sp
com
me
ts
4v
DVN
vl
XII
-13.8
C
Gr
Cu
AP
sp
me
com
DVN
4v
vl
-13.6
XII
D
gel
Cu
me
4v
DVN
vl
XII
-13.3

Table 1
Primers used for amplification of AMPA receptor subunit cDNA

Subunit		Primer sequence 5′ –3′	Position	GenBank accession no.
GluR1–4	For	CCTTTGGCCTATGAGATCTGGATGTG	1797–2545	X17184
	Rev	TCGTACCACCATTTGTTTTTCA		
GluR1	For	AGAAAAGAGCCGGCAGAGCA	95–815	X17184
	Rev	TGATTCACAGTCAACCACCA		
GluR2	For	GAGGAGCAAATGTCTCTGGA	1072–1692	M85035
	Rev	GAACCCACAGTGTTTGGCAA		
GluR3	For	GAAAACCCAATGGTTCAGCA	973–1493	M85036
	Rev	CATTTCCTTCCAGCTGCTCA		
GluR4	For	CTCTGGGCAATGACACAGCA	1371–1791	M85037
	Rev	CCAGAGGGTCCAAGAAGGAA		
GAPDH	For	ACAACTTTGGCATCGTGGAA	1339–1559	AF106860
	Rev	TTGGGGGTAGGAACACGGAA		
GAPDH	For	TGATGACATCAAGAAGGTGGTGAAG	789–1028	NM_017008
	Rev	TCCTTGGAGGCCATGTAGGCCATG		

trations, annealing temperatures and cycle number, whereby the reaction remained within the exponential phase, up to 34 cycles (Fig. 2). All determinations were performed at least three times from the same samples of cDNA, and PCR products for each subunit from SH and WKY rats were run on the same gel. Monochrome photographs of the gels were digitally scanned and imported as JPEG files into Adobe Photoshop 5. The mean pixel density of each AMPA subunit band and its GAPDH control was measured and analysed using the NIH ImageJ computer program version 1.2 (http://rsb.info.nih.gov/nih-image). Each AMPA subunit value was normalised to the corresponding GAPDH band from the same lane and results for individual subunits from the six rats were averaged. Each SH result was then compared to its own WKY control. For clarity, the WKY control was adjusted to have a relative expression of one and the SH result normalised accordingly. The SH and WKY values were compared using a Student's unpaired *t*-test.

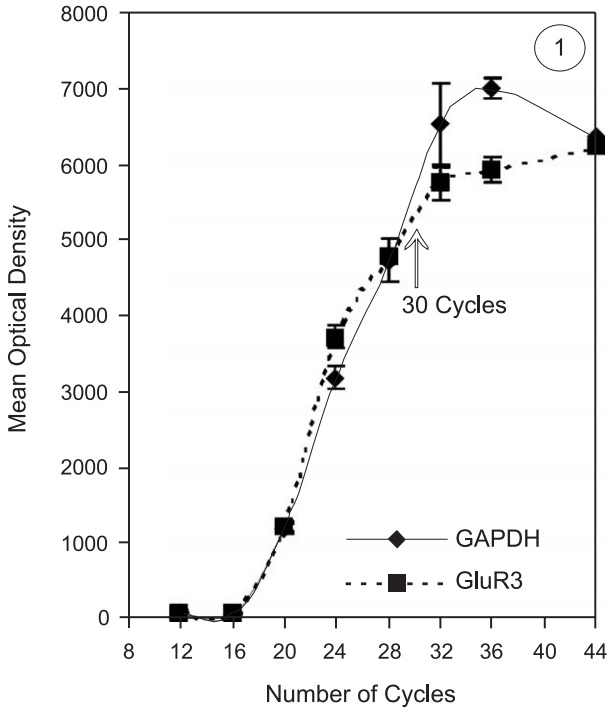

Fig. 2. Kinetics of the amplification of GAPDH (♦) and GluR3 (■) mRNAs. PCR products were separated on 2% agarose gels and subjected to densitometric analysis using the NIH ImageJ computer program. The graph shows the linear and plateau phases of amplification. Subsequent reactions for semi-quantitative analysis were carried out in the linear phase at 30 cycles (↑).

2.5. Immunohistochemistry

Adult male Wistar, SH and age-matched (12-week) WKY rats ($n = 6$ each) weighing 200–230 g were perfused with 4% paraformaldehyde and 0.1% glutaraldehyde in 0.1 M phosphate buffer. Coronal 30 μm brainstem sections were incubated in affinity-purified rabbit antisera to synthetic peptides corresponding to C-terminal sequences of GluR1, GluR2, GluR2/3 and GluR4 (Chemicon, Harrow, Middx, UK), shown to be specific for their receptor subunits by Western blot analysis of membranes transfected with GluR1, 2, 3 or 4 cDNAs [54]. All antibodies were diluted 1:150 in PBS containing 0.1% Triton X-100, and visualised by a biotin–avidin–peroxidase method as previously described [36]. Sections from WKY and SH were processed concurrently under standardised conditions (reagent dilutions, incubation and wash times, temperature). Labelled sections were examined on a Zeiss Axioskop microscope and digital images captured with an Acquis imaging system (Synoptics, Cambridge, UK).

The mean areas of the NTS in WKY and SH brains ($n = 4$ each) were determined on histologically stained sections at three transverse levels (approximately bregma −14.3, −14.0 and −13.7mm [30]) using the Acquis measurement software. The immunolabelling intensities for GluR1, GluR2, GluR2/3 and GluR4 were quantified using the ImageJ densitometric analysis software in images captured at ×40 from selected areas (each 0.01 mm^2) of the dorsomedial medulla (commissural, interstitial, medial subnuclei of NTS, dorsal vagal nucleus, hypoglossal motor nucleus) at the same three levels of sectioning.

3. Results

3.1. Analysis of AMPA receptor subunit expression by RT-PCR

3.1.1. Sampling of NTS tissue

Examination of sections from slices of the brain stem after collecting tissue punches verified that the placement of the punches in the NTS was accurately located and centred on the medial subnucleus (Fig. 1). The majority of the tissue collected was from within the confines of the NTS, with a small amount of contamination from the dorsal vagal nucleus (DVN) and ventral edge of the gracile nucleus.

3.1.2. Total AMPA receptor subunit expression

RT-PCR analysis of RNA from both NTS and cerebellum of Wistar rats produced a single DNA band (Fig. 3A) that corresponded to the predicted size of the Glu1–4 cDNAs (749 bp). RNA samples without reverse transcription, or water with primers produced no detectable product. The specificity of the GluR1–4 products was confirmed by the restriction site analysis using endonuclease enzymes, which

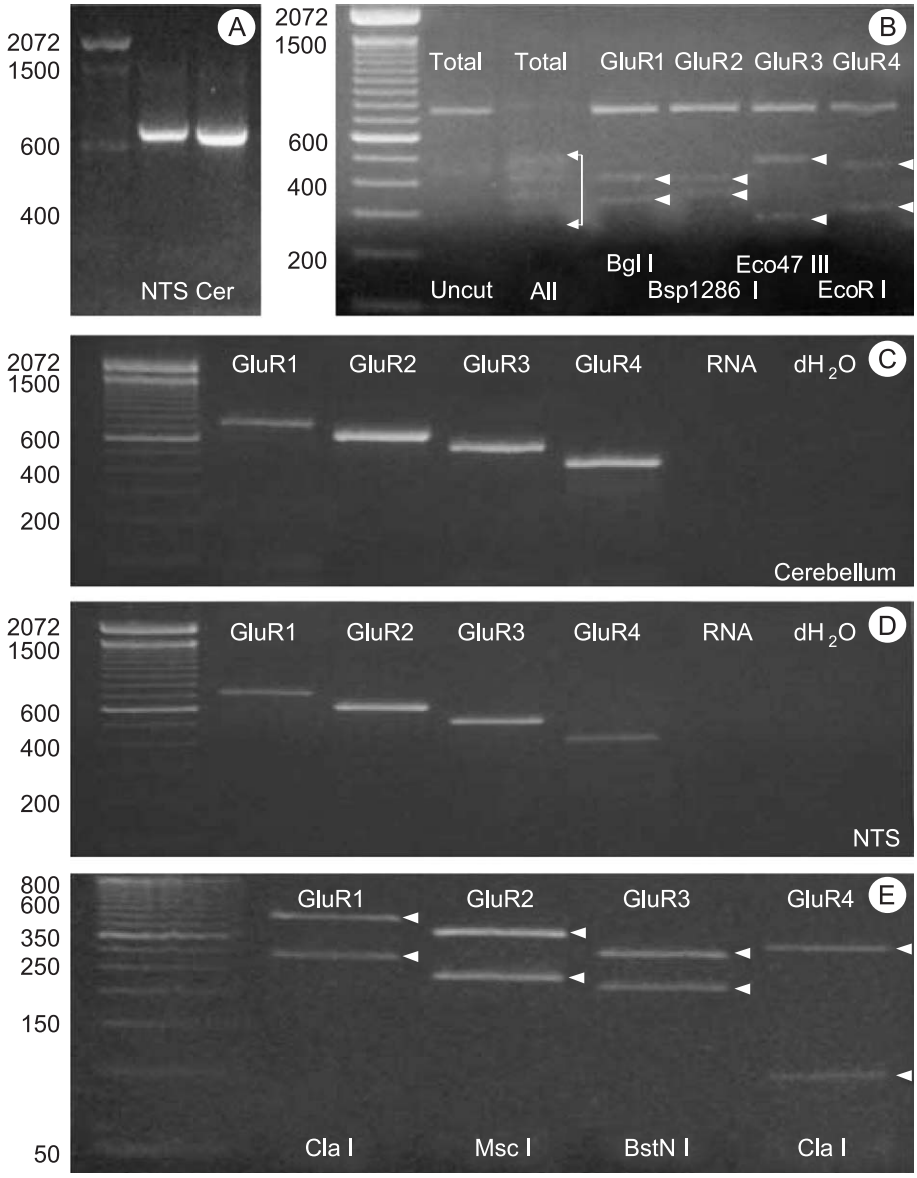

Fig. 3. RT-PCR analysis of total AMPA (GluR1–4) receptor mRNAs in cerebellum and NTS tissue (A). Amplification was performed using primers common to all four AMPA subunits yielding a product of 749 bp in both tissues when separated on a 2% agarose gel. Restriction enzyme digest using endonuclease enzymes specific for each of the subunits confirmed the identity of the PCR products (B). Two fragments matching the predicted size were produced for each subunit; the remaining 749 bp band corresponds to amplified fragments left uncut by the restriction digest. Expression of the individual AMPA receptor subunits in the cerebellum (C) and NTS (D) was examined using primers specific for each subunit. Amplicons representing GluR1 (720 bp), GluR2 (620 bp), GluR3 (520 bp) and GluR4 (420 bp) were present in both tissues and were confirmed by the presence of two bands following restriction enzyme digest and separation on a 4% agarose gel (E).

in all cases produced bands that had the size predicted for the restriction digests of the GluR1, 2, 3 or 4 amplified fragments (Fig. 3B). This demonstrated that the mRNAs for all four subunits (GluR1–4) were present in the rat NTS.

3.1.3. Expression of individual AMPA receptor subunits

To further confirm that each GluR subunit is expressed in the NTS, RT-PCR analysis was performed using individual GluR1–4 primers. In control tissue from the cerebellum, a single PCR band was observed for each primer pair that matched the predicted sizes of the GluR1–R4 subunits, 720, 620, 520 and 420 bp, respectively (Fig. 3C). In NTS tissue, all AMPA receptor subunits were similarly detected (Fig. 3D).

The specificity of the PCR products was again confirmed by restriction site analysis (Fig. 3E). DNA sequencing provided further verification of the veracity of the AMPA subunit PCR products.

3.2. Semi-quantitative PCR of AMPA receptor mRNA in SH and WKY

In order to control for possible size difference in the brains between SH and WKY, the mean weights of the rats were calculated and compared. The weights of the SH rats (226 ± 18 g, mean ± S.E., $n = 6$) and WKY rats (212 ± 21 g) were not found to be significantly different (Student's unpaired *t*-test). Furthermore, the mean areas of NTS tissue determined from histological sections were not significantly different.

3.2.1. Total AMPA receptor subunits

RT-PCR analysis detected strong expression of AMPA (GluR1–4) receptors in the NTS of both the SH and WKY rats. Co-amplification of GluR1–4 and GAPDH produced bands of anticipated size (749 and 239 bp, respectively, Fig. 4A). The expression of total AMPA receptor mRNA in the NTS of SH animals was found to be significantly greater than the expression in WKY animals ($p < 0.005$, Student's paired *t*-test).

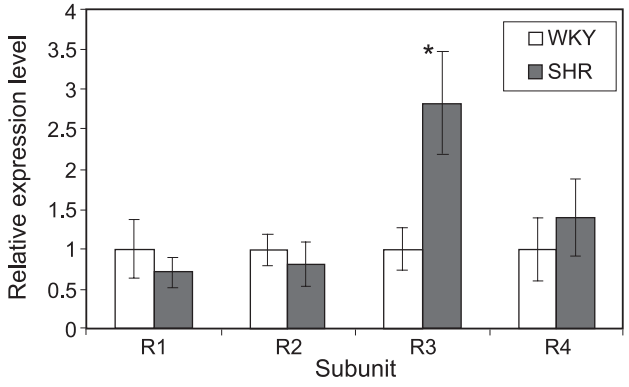

Fig. 5. Relative expression levels of individual AMPA receptor subunit mRNAs in the NTS of SH and WKY rats ($n = 6$). Each subunit is compared to its GAPDH control, which has been adjusted to have an expression level of 1. All results are the mean ± standard error mean and were subjected to a Student's unpaired *t*-test, $*p = 0.003$.

3.2.2. Individual AMPA receptor subunits

Semi-quantitative PCR analysis detected strong expression of all the AMPA receptor subunits in the NTS of both the SH and WKY rats. Co-amplification of the AMPA subunit with GAPDH produced bands of the anticipated sizes (Fig. 4B). The GluR1, GluR2 and GluR4 subunits did not show any significant changes in the levels of expression between the WKY and SH animals (Fig. 5). However, the data indicated a significant increase in the level of expression of GluR3 mRNA in SH compared to the WKY controls ($p = 0.003$, Student's unpaired *t*-test). In tissue samples from the cerebral cortex or cerebellum, no differences in the level of AMPA subunit expression between SH and WKY were seen.

3.3. Localisation of receptors by immunohistochemistry

3.3.1. GluR1 immunoreactivity

Immunolabelling for GluR1 in the dorsomedial medulla was heterogeneously distributed. Intense labelling of cells

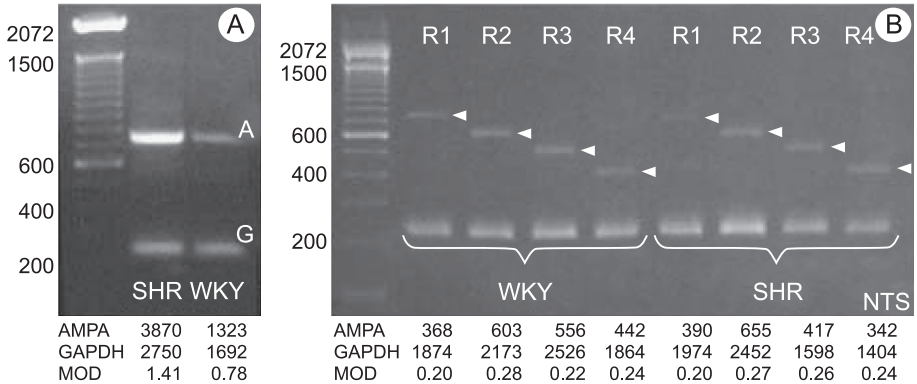

Fig. 4. Co-amplification of total AMPA receptor mRNA in the presence of primers for the 'house-keeping' gene GAPDH yielded two bands of anticipated size in NTS tissue extracted from SH and WKY rats (A). Note that the intensity of the band produced by the GluR1–4 primers is higher in the SH rat compared to the WKY rat when normalised to its GAPDH control. Results for the co-amplification of the individual subunits with GAPDH also generated two bands that corresponded to their predicted size (B). Pixel density measurements are included for each subunit, the GAPDH control and the normalised results. For semi-quantitative analysis, results for individual subunits in all SH and WKY samples were resolved on the same agarose gel. Mean pixel density measurements (MOD) are included for each subunit.

and neuropil was present throughout the area postrema and extended into the subpostremal, commissural, medial and dorsomedial NTS (Fig. 6A). In the interstitial subnucleus, scattered fusiform and ovoid neurones and their strongly stained dendrites extended into the neuropil between the fascicles of the tractus solitarius (Fig. 6E). Somata with weak or moderate immunoreactivity had a widely scattered distribution in remaining areas of the NTS. Very strongly labelled bipolar and multipolar cells occurred in the area bounded by the ventrolateral NTS, the lateral tip of the DVN and the hypoglossal nucleus, and the dorsal reticular area, most probably corresponding to the nucleus interme-

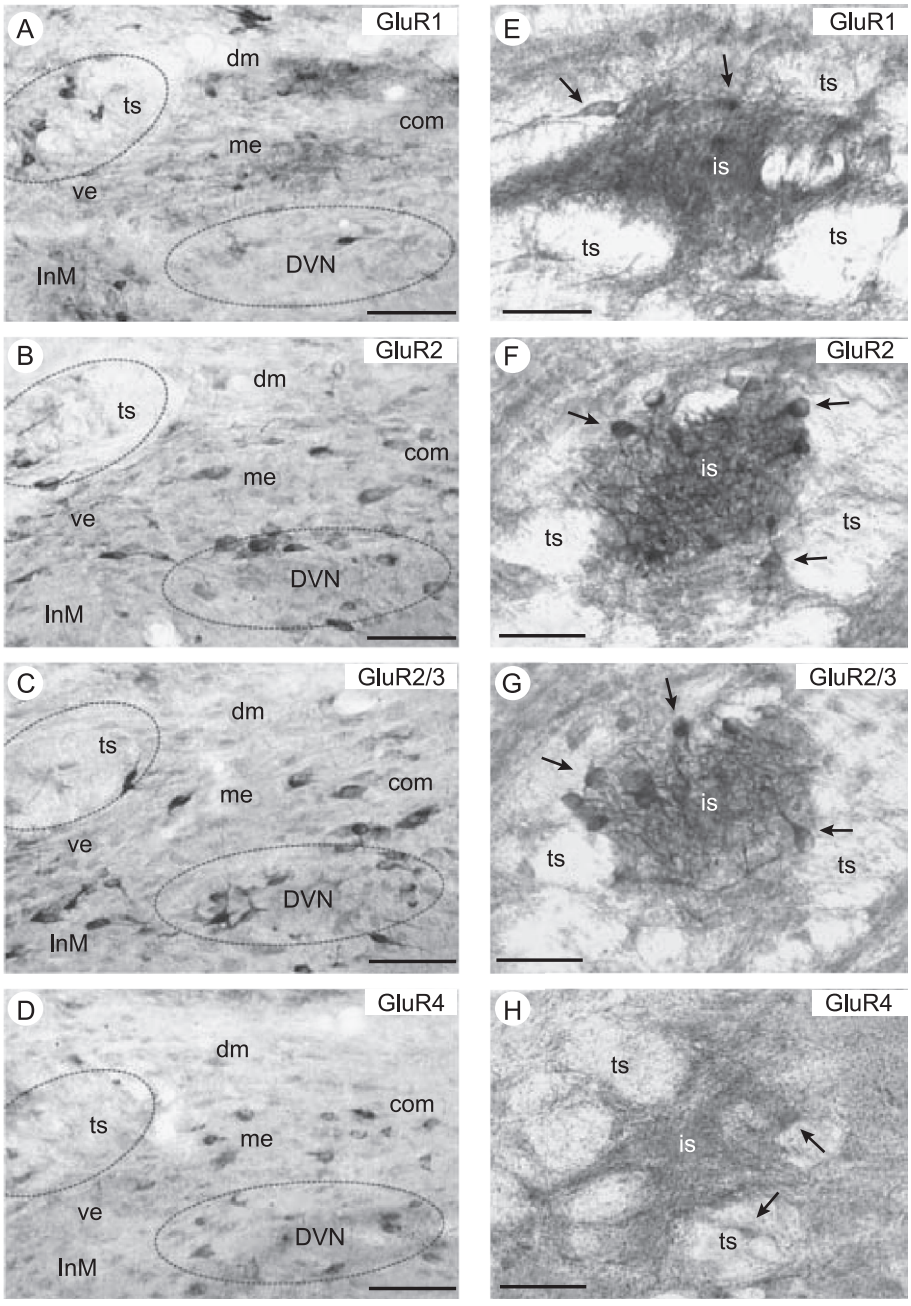

Fig. 6. Neurones in the NTS of Wistar rat immunoreactive for GluR1 (A, E), GluR2 (B, F), GluR2/3 (C, G) and GluR4 (D, H). (A–D) Serial sections of caudal NTS at a coronal level corresponding to bregma − 14.3 mm [30], contrasting labelling patterns with the four AMPA subunit antibodies. (A) Relatively few strongly GluR1 immunoreactive cells are present in NTS, with the most intensely labelled cell groups located in the dorsomedial (dm) and medial (me) subnuclei, tractus solitarius (ts, outlined) and nucleus intermedius (InM). (B) Group of strongly GluR2 immunoreactive cells seen in the ventral (ve) and commissural (com) subnuclei, as well as the dorsal vagal nucleus (DVN, outlined). (C) The GluR2/3 antibody gives a broadly similar pattern of labelling to that seen for GluR2. (D) Light to moderate GluR4 labelling present in many cells scattered throughout all subdivisions of NTS and DVN. Panels E–H show the different patterns of labelling given by the subunit-specific antibodies in cell somata (arrows) and neural processes in the interstitial subnucleus (is) surrounded by fascicles of the ts, at a more rostral level of sectioning (bregma − 13.8 mm). Scale bars 100 μm in A–D, 50 μm in E–H.

dius (Fig. 7A). Very few neurones in the DVN were labelled for GluR1.

3.3.2. GluR2 immunoreactivity

The GluR2 specific antibody produced a variable light to intense labelling in many cells throughout the commissural, medial, central, ventral and dorsomedial NTS at all rostro-caudal levels (Fig. 6B). Especially distinct labelling of neurones and their dendritic processes was evident in the interstitial (Fig. 6F) and other clusters of well-labelled cells were found in the ventrolateral subnucleus at caudal levels and more rostrally in the central subnucleus. Less strongly labelled cells and fibres were observed in the area postrema. Small cells with fine processes, probably corresponding to astrocytes, were sometimes seen in the medial NTS and DVN, and labelling was consistently seen in tanycyte-like

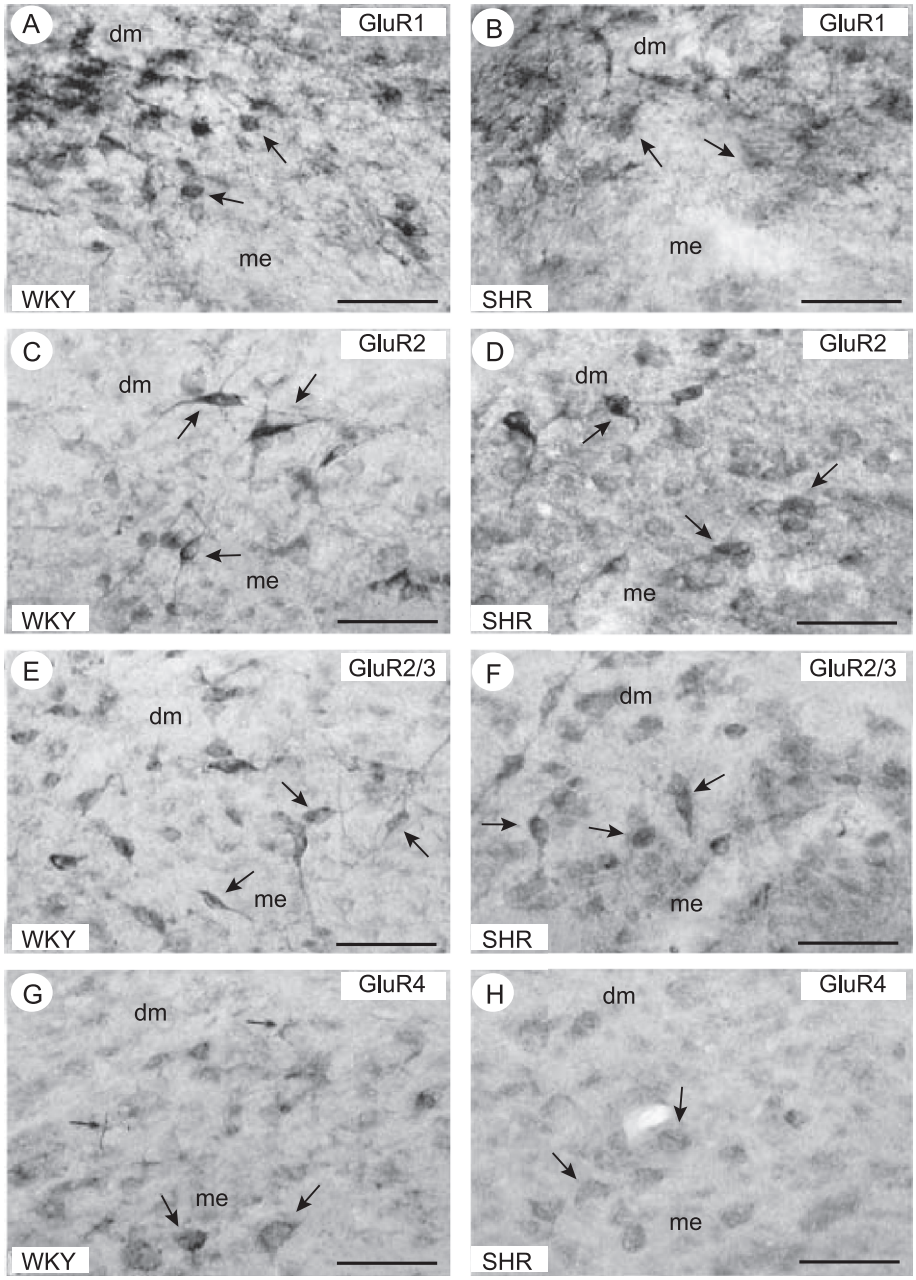

Fig. 7. Distribution of immunoreactivity for the AMPA receptor subunits in the NTS at the area postrema level (bregma − 13.6 mm [30]) in WKY (A, C, E, G) and SH (B, D, F, H) rats. Sections from WKY and SH were labelled simultaneously, under the same conditions. Greater numbers of strongly GluR1 immunoreactive cell bodies (arrows) are seen in the dorsomedial NTS (dm) in WKY (A) compared to SH (B). With both the GluR2 (C) and GluR2/3 (E) specific antibodies, intensely labelled neurones with visible dendrites (arrows) are seen in the dorsomedial and medial (me) subnuclei in WKY, whereas in SH (D and F) labelling of somata and proximal dendrites is less intense and more labelled punctata are visible in the neuropil. With the GluR4 antibody, a slight increase in the number of cells showing granular labelling is observed in the medial NTS (me) of SH (H) compared to WKY (G), but fewer strongly immunoreactive cells are seen. Note labelling of astrocytes for GluR4 (double headed arrows in G). Scale bars = 50 μm.

ependymal cells along the interface of the area postrema with the NTS. Neuronal labelling was moderately strong in many of the DVN neurones (Fig. 6B).

3.3.3. GluR2/3 immunoreactivity

The antibody directed against the GluR2 and GluR3 common sequences produced a pattern of labelling almost identical to that seen with the GluR2 antibody (Fig. 6C), but the number of intensely labelled neurones and their dendritic processes in the central, medial and commissural NTS was clearly greater. As for GluR2, the most prominent and strongly labelled group of cells was seen in the interstitial subnucleus of the NTS (Fig. 6G). Most of the immunostained structures appeared to be neuronal rather than glial, but were so densely packed that they could often not be conclusively identified as corresponding to axons, their terminals or dendritic profiles.

3.3.4. GluR4 immunoreactivity

With GluR4 antibodies, labelling of cell bodies was most clearly seen in the medial and the commissural NTS (Fig. 6D). Many lightly labelled cells were scattered throughout the other subnuclei of the NTS, with their labelling intensity generally increased at rostral levels compared to caudal levels. A diffuse, but intense labelling of fibres and punctata was present in the neuropil, possibly representing dendritic profiles or glial processes. This labelling was particularly strong in the interstitial subnucleus, but few clearly labelled neurones could be discriminated (Fig. 6H).

3.4. Immunolocalisation of AMPA receptor subunit proteins in NTS of SH and WKY

For the GluR1 receptor subunit, the neuronal staining in much of the rostral and ventrolateral parts of the NTS and area postrema was very similar in both strains. Despite the labelling of somata and their proximal dendrites in the medial, dorsomedial and commissural subnuclei of the caudal NTS appearing to be more distinct in WKY compared to SH (Fig. 7A,B), there were no significant differences in labelling intensity revealed by densitometric analysis (Table 2).

There were similar differences in the staining pattern for GluR2 and 2/3 subunits in the medulla in SH and WKY. Again, neuronal perikarya with distinct dendritic processes were intensely labelled against a lightly labelled neuropil in the commissural, interstitial, dorsomedial, medial and central subnuclei in the WKY rat, but in the corresponding areas in SH rats cellular labelling was less distinct against a more heavily labelled neuropil with both the antibodies used (Fig. 7C–F). This subjective difference for GluR2/3 was supported by the densitometric analysis, which showed a significantly higher intensity of labelling in the commissural and medial NTS, and also the DVN in the SH rat (Table 2). There were, however, no quantitative differences in the density of labelling in the NTS with the GluR2 specific antibody (Table 2).

Table 2
Quantitation of GluR immunolabelling in dorsomedial medulla (arbitrary pixel density units, mean ± S.E.M.)

Parameter	WKY	SH
Rat body weight (g)	228.5 ± 11.2	222.3 ± 14.3
Area of entire NTS (mm^2)	0.236 ± 0.006	0.209 ± 0.004
GluR1 labelling intensity		
Commissural NTS	104.7 ± 1.1	99.8 ± 1.8
Medial NTS	101.2 ± 3.1	95.0 ± 1.8
Interstitial NTS	122.6 ± 9.0	112.7 ± 6.6
Dorsal vagal nucleus	86.5 ± 2.5	86.5 ± 2.9
Hypoglossal nucleus	79.1 ± 3.9	76.9 ± 6.3
GluR2 labelling intensity		
Commissural NTS	87.4 ± 2.4	88.8 ± 9.1
Medial NTS	94.7 ± 3.8	91.5 ± 5.0
Interstitial NTS	124.7 ± 6.7	128.9 ± 5.6
Dorsal vagal nucleus	113.5 ± 3.6	97.0 ± 5.3*
Hypoglossal nucleus	78.0 ± 5.5	83.5 ± 5.8
GluR2/3 labelling intensity		
Commissural NTS	60.9 ± 3.5	91.4 ± 7.4*
Medial NTS	81.1 ± 1.5	107.1 ± 2.7**
Interstitial NTS	125.7 ± 3.6	115.6 ± 6.4
Dorsal vagal nucleus	66.1 ± 0.7	84.0 ± 1.4**
Hypoglossal nucleus	80.4 ± 0.5	85.3 ± 2.0
GluR4 labelling intensity		
Commissural NTS	66.6 ± 3.3	58.7 ± 2.4
Medial NTS	68.4 ± 1.6	67.1 ± 3.9
Interstitial NTS	92.5 ± 4.9	81.9 ± 3.4
Dorsal vagal nucleus	68.6 ± 1.8	68.3 ± 5.3
Hypoglossal nucleus	74.4 ± 1.1	82.7 ± 3.3

* Significantly different from WKY value at $p < 0.05$ (unpaired Student t-test).

** Significantly different from WKY value at $p < 0.01$ (unpaired Student t-test).

With the GluR4 antibody, light to moderate granular staining for GluR4 could be seen in neuronal projections as well as cell bodies throughout the commissural, dorsomedial and medial subnuclei in SH rats. In WKY, the labelling was characterised by diffuse staining of apparently fewer neuronal and glial cell bodies that was more variable in intensity than in SH (Fig. 7G,H). No quantitative differences in staining density between SH and WKY brains were detected (Table 2).

4. Discussion

By using a semi-quantitative PCR method, we have shown for the first time that the level of total AMPA receptor mRNA expression, and in particular that for GluR3 subunit is significantly higher in the NTS of the SH compared to the WKY rat. This difference was reflected by a changed pattern of tissue labelling for the individual receptor subunit proteins observed using specific antibodies. In other brain areas analysed, there was no difference in GluR3 expression between SH and WKY. This data indicates a possible role for changed AMPA receptor gene expression in NTS tissue in the pathogenesis of hypertension in SH.

4.1. Semi-quantitative analysis of AMPA subunit expression: methodological aspects

The sizes of the amplified fragments produced by PCR on RNA samples from NTS tissue corresponded to the predicted sizes for the GluR1–4 subunit cDNAs, and the veracity of the products was confirmed by restriction enzyme digestion and sequencing, suggesting that these receptor subunit proteins are expressed on NTS neurones. Our method allowed us to accurately and consistently sample tissue from the same area of the NTS. The placement of the punches was not affected by differences in the body weights or brain sizes between SH and WKY, which were found not to be significantly different at 12 weeks, despite the fact that by this age, differences between the two strains in blood pressure and central cardiovascular reflexes are already developed [12,15,25,53]. Although a relatively pure preparation of NTS tissue can be obtained from tissue punches, it is important to note that one cannot avoid extracting RNA from the DVN neurones that lie adjacent to the NTS and have large dendrites ascending into the medial NTS.

The semi-quantitative PCR protocol employed in this study is a variation on previously reported densitometric methods, which have measured mRNA expression by co-amplification with a "house-keeping" gene as an internal standard [10,37]. The ubiquitous, constitutively expressed GAPDH has been used in many semi-quantitative PCR studies as an internal standard, as its expression level is believed not to vary with physiological conditions [34,37,46].

Assuming that the relative abundance of the PCR amplicons is indicative of the relative expression of their mRNAs in the NTS tissue samples, the levels of expression of total AMPA receptors, and specifically of the GluR3 subunit, were found to be significantly higher in SH than in WKY. It is likely that a difference of such magnitude in mRNA expression could indicate differences in functional receptor proteins inserted into cell membranes between the two strains correlated with differences in blood pressure. However, these data must be interpreted with caution. Although the SH, compared with inbred normotensive WKY controls, is widely accepted as an animal model for essential hypertension, there are chemical and anatomical differences in the brains of the two strains that do not directly involve areas concerned with blood pressure control [29,40,42]. Such differences are possibly indicative of substantial genetic variation between the strains.

5. Immunolabelling in Wistar rat

The distributions of immunoreactivity for the GluR1–4 subunits that we observed in the NTS are similar to those described in earlier immunohistochemical studies using specific antibodies recognising C-terminal peptide sequences of the AMPA subunits [2,3,18,20,32] and hybridization studies [38], although there are some notable differences. Previous studies reported that antibodies to GluR1, GluR2 and GluR2/3 produced intense staining in neurones of different sizes and morphologies generally in accordance with our observations, whereas staining for GluR4 was restricted mainly to smaller, probably glial cells. This correlated with the moderate to high levels of mRNA for GluR1 and GluR2, and relatively low levels of mRNA for GluR3 and GluR4 detected in the rat NTS by in situ hybridization [38]. The GluR2 subunit is widely expressed in the CNS and has been demonstrated to confer Ca^{2+} impermeability to AMPA receptors, but was previously thought to have relatively weak expression levels in brain stem neurones [7,31,33]. However, recent studies have revealed strong expression of GluR2 in a subset of NTS neurones [18,20], in agreement with our present results. We observed only minor differences between the pattern of labelling with the GluR2 specific antibody and the antibody raised against the common C-terminal sequence of GluRs 2 and 3. This could indicate that expression of GluR2 subunit proteins throughout the NTS predominates over GluR3, as suggested by the results of in situ hybridisation studies [38]. Alternatively, the GluR3 subunit might be extensively colocalised in NTS cells expressing GluR2. In the only immunohistochemical study so far performed with a GluR3 specific antibody, co-expression of GluR3 with GluR2 was observed in the hippocampus, but many GluR3 positive interneurones lacked GluR2 immunoreactivity [27].

5.1. Immunolabelling in SH and WKY rats

Our light microscopic immunohistochemical investigation revealed some consistent differences in the distribution of the four AMPA receptor subunit proteins between adult SH and age-matched WKY rats, which correlated well with the PCR findings. The labelling intensity of the neuropil relative to neuronal somata with GluR1, GluR2 and GluR2/3 antibodies appeared to be increased in specific areas of the caudal NTS in SH compared to WKY. Densitometric analysis revealed an increase in the overall intensity of GluR2/3 antibody immunolabelling in the NTS of the SH rats, but there was no significant differences in the labelling with the GluR1, GluR2 or GluR4 antibodies. Since electron microscopic studies have revealed that much of the AMPA receptor labelling in perikarya seen at light microscopic level with C-terminal directed antibodies represents an intracellular pool of receptor that is probably not functional in synaptic transmission [18], our findings could be interpreted as indicating that in the NTS of the SH the proportion of functional GluR1–3 proteins in the distal dendritic compartment is increased, by either increased mRNA expression or a redistribution of receptors associated with hypertension. This supposition is in agreement with the observations of previous studies that provided ultrastructural evidence that GluR1 immunoreactivity is preferentially associated with small dendritic profiles in the NTS [2],

and that the number of such labelled dendritic structures is increased in the medial NTS of SH compared to age-matched WKY rats [1], suggesting that postsynaptic AMPA receptor distribution in NTS neurones may be altered by chronic elevations in arterial pressure. However, the same authors found no difference in the distribution of GluR2/3 immunoreactivity, which was preferentially localised to pre- and post-synaptic neuronal sites [1,2] contrary to our present findings from both PCR and immunohistochemistry. In contrast to our results, Ashworth-Preece et al. [6], using autoradiographic methods, found no difference in total AMPA receptor binding density in the NTS between the two strains of rat.

5.2. Functional significance of increased AMPA receptor expression in SH

The main areas of the caudal NTS in which we observed differences in the labelling pattern between SH and WKY rats, i.e. the commissural, medial and dorsomedial subnuclei, are believed to be the area primarily involved in cardiovascular regulation. Although the various sensory inputs to NTS (cardiovascular, respiratory, gastrointestinal and gustatory) are only loosely segregated viscerotopically to subnuclei along the rostral–caudal extent of NTS [23], this caudal medial subdivision, underlying the area postrema and medial to the tractus solitarius, has been shown to receive terminations from baroreceptor and cardiac afferent fibres [11]. Numerous glutamate-immunoreactive terminals have been shown to synapse onto neurones in this area of the NTS, and these include vagal afferent fibre terminals [35,47]. Many other biochemical studies provide evidence that glutamate is released from the terminals of vagal primary afferent fibres to excite NTS neurones [5,22,49,51]. When microinjected into the caudal NTS in vivo, glutamate produces hypotensive and bradycardic responses similar to those observed on baroreceptor fibre [51] or cardio-pulmonary fibre [52] activation. Exogenously applied glutamate is capable of acting on NTS neurones via NMDA, non-NMDA and metabotrophic receptors, but with non-NMDA mechanisms predominating in the transmission of afferent information onto second-order baroreceptive neurones [13,14,39]. Recent combined pharmacological and *c-fos* expression studies have confirmed that AMPA receptors, including the GluR1 and/or GluR2 subunits, are involved in the activation of second-order NTS neurones on baroreceptor stimulation, whereas NMDA receptors are likely to mediate the activation of higher-order NTS neurones [8,9,56].

The cardiovascular responses to glutamate or agonists applied to the NTS in SH and WKY rats have been compared in only one study, but this showed a shift to the right in the arterial pressure dose–response curve to glutamate in the SH [50], suggesting a reduced sensitivity of NTS neurones to glutamate. This is possibly due to a desensitisation or down-regulation of receptors, since the concentration of glutamate in NTS tissue was found to be significantly higher in SH than WKY [19]. There is also pharmacological and anatomical evidence for differences in the glutamatergic systems of the caudal ventrolateral medulla and rostral ventrolateral medulla between SH and WKY rats [16,26,41,48,55]. These differences can be interpreted as indicating a reduced excitatory output from the NTS to GABAergic neurones in the ventrolateral medulla that tonically inhibit the sympathetic vasomotor neurones, resulting in elevated blood pressure. Thus, the hypertensive condition may be characterised by changes in glutamatergic transmission at several different levels of the cardiovascular reflex pathways within the brainstem. Such changes may involve plasticity of AMPA receptor subunit expression in the NTS. For example, increased expression of GluR3 compared to GluR2 may result in an increase in Ca^{2+} permeability of AMPA receptors and a predisposition of NTS neurones to excitotoxic effects. However, whether such a mechanism contributes to the development of hypertension in SH, or is secondary to changes in glutamate metabolism and release, or even changes in other transmitter systems as a consequence of raised blood pressure remains to be established.

Acknowledgements

This study was supported by project grants from the British Heart Foundation and a Medical Research Council studentship awarded to E.J.S.

References

[1] S.A. Aicher, J.A. Kraus, A. Patel, S. Sharma, AMPA-type glutamate receptor density is increased in the nuclei of the solitary tract (NTS) of spontaneously hypertensive rats, Soc. Neurosci. Abstr. 25 (1999) 11.10.

[2] S.A. Aicher, S. Sharma, J.L. Mitchell, Co-localization of AMPA receptor subunits in the nucleus of the solitary tract of the rat, Brain Res. 958 (2002) 454–458.

[3] R. Ambalavanar, C.L. Ludlow, R.J. Wenthold, Y. Tanaka, M. Damirjian, R.S. Petralia, Glutamate receptor subunits in the nucleus of the tractus solitarius and other regions of the medulla oblongata in the cat, J. Comp. Neurol. 402 (1998) 75–92.

[4] M.C. Andresen, D.L. Kunze, Nucleus tractus solitarius—gateway to neural circulatory control, Annu. Rev. Physiol. 56 (1994) 93–116.

[5] M.C. Andresen, M.Y. Yang, Non-NMDA receptors mediate sensory afferent synaptic transmission in medial nucleus tractus solitarius, Am. J. Physiol. 259 (1990) H1307–H1311.

[6] M.A. Ashworth-Preece, F. Chen, B. Jarrott, A.J. Lawrence, Visualisation of AMPA binding sites in the brain stem of normotensive and hypertensive rats, Brain Res. 834 (1999) 186–189.

[7] B. Bettler, C. Mulle, Review: neurotransmitter receptors: II. AMPA and kainate receptors, Neuropharmacology 34 (1995) 123–139.

[8] J.Y. Chan, W.C. Chen, H.Y. Lee, S.H. Chan, Elevated Fos expression in the nucleus tractus solitarii is associated with reduced baroreflex response in spontaneously hypertensive rats, Hypertension 32 (1998) 939–944.

[9] J.Y.H. Chan, S.M. Yang, S.H. Chan, Mediation by *N*-methyl-D-aspartate and non-*N*-methyl-D-aspartate receptors in the expression of Fos protein at the nucleus tractus solitarii in response to baroreceptor activation in the rat, Neuroscience 83 (1998) 93–105.

[10] L. Chen, D.M. Segal, D.C. Mash, Semi-quantitative reverse-transcriptase polymerase chain reaction: an approach for the measurement of target gene expression in human brain, Brain Res. Protoc. 4 (1999) 132–139.
[11] J. Ciriello, S.L. Hochstenbach, S. Roder, Central projections of baroreceptor and chemoreceptor afferent fibres in the rat, in: I.R.A. Barraco (Ed.), Nucleus of the Solitary Tract, CRC Press, Boca Raton, 1994, pp. 35–50.
[12] J.G. Dickhout, R.M.K.W. Lee, Blood pressure and heart rate development in young spontaneously hypertensive rats, Am. J. Physiol. 274 (1998) H794–H800.
[13] C.M. Foley, J.A. Moffitt, M. Hay, E.M. Hasser, Glutamate in the nucleus of the solitary tract activates both ionotropic and metabotrophic glutamate receptors, Am. J. Physiol. 275 (1998) R1858–R1866.
[14] F.J. Gordon, C. Leone, Non-NMDA receptors in the nucleus of the tractus solitarius play the predominant role in mediating aortic baroreceptor reflexes, Brain Res. 568 (1991) 319–322.
[15] G.A. Head, M.A. Adams, Characterization of the baroreceptor heart rate reflex during development in spontaneously hypertensive rats, Clin. Exp. Pharmacol. Physiol. 19 (1992) 587–597.
[16] V. Kapoor, R. Kapoor, J.P. Chalmers, Altered responsiveness of medullary depressor neurones to L-glutamate and D-serine in SH rats, NeuroReport 7 (1996) 1409–1412.
[17] K. Keinanen, W. Wisden, B. Sommer, P. Werner, A. Herb, T.A. Verdoorn, B. Sakmann, P.H. Seeburg, A family of AMPA-selective glutamate receptors, Science 249 (1990) 556–560.
[18] J.P. Kessler, A. Baude, Distribution of AMPA receptor subunits GluR1–4 in the dorsal vagal complex of the rat: a light and electron microscope immunocytochemical study, Synapse 34 (1999) 55–67.
[19] T. Kubo, M. Kihara, Y. Misu, Altered amino acid levels in brainstem regions of spontaneously hypertensive rats, Clin. Exp. Hypertens., Part A Theory Pract. 11 (1996) 233–241.
[20] O. Lacassagne, J.P. Kessler, Cellular and subcellular distribution of the amino-3-hydroxy-5-methyl-4-isoxazole propionate receptor subunit GluR2 in the rat dorsal vagal complex, Neuroscience 99 (2000) 557–563.
[21] B. Lambolez, E. Audinat, P. Bochet, F. Crépel, J. Rossier, AMPA receptor subunits expressed by single Purkinje cells, Neuron 9 (1992) 247–258.
[22] A.J. Lawrence, B. Jarrott, Neurochemical modulation of cardiovascular control in the nucleus tractus solitarius, Prog. Neurobiol. 48 (1996) 21–53.
[23] A.D. Loewy, Central autonomic pathways, in: A.D. Loewy, K.M. Spyer (Eds.), Central Regulation of Autonomic Functions, Oxford Univ. Press, New York, 1990, pp. 88–103.
[24] M. Mansour, N. Nagarajan, R.B. Nehring, J.D. Clements, C. Rosenmund, Heteromeric AMPA receptors assemble with a preferred subunit stoichiometry and spatial arrangement, Neuron 32 (2001) 841–853.
[25] N. Minami, G.A. Head, Cardiac vagal responsiveness during development in spontaneously hypertensive rats, Auton. Neurosci.: Basic Clin. 82 (2000) 115–122.
[26] M. Miura, K. Takayama, J. Okada, Difference in sensitivity of cardiovascular and respiratory control neurons in the subretrofacial nucleus to glutamate receptor subtype agonists in SH, WKY and cats, J. Auton. Nerv. Syst. 36 (1991) 1–12.
[27] D. Moga, P.R. Hof, P. Vissavajjhala, T.M. Moran, J.H. Morrison, Parvalbumin-containing neurons in rat hippocampus have an AMPA receptor profile suggestive of vulnerability to excitotoxicity, J. Chem. Neuroanat. 23 (2002) 249–254.
[28] D.T. Monaghan, R.J. Bridges, C.W. Cotman, The excitatory amino acid receptors: their classes, pharmacology, and distinct properties in the function of the central nervous system, Annu. Rev. Pharmacol. Toxicol. 29 (1989) 365–402.
[29] D.K. Nelson, R.L. Coulson, J.H. Myers, R.A. Browning, Neuroanatomical differentiation in the brain of the spontaneously hypertensive rat (SH): I. Volumetric comparisons with WKY control, Clin. Exp. Hypertens. 15 (1993) 867–894.
[30] G. Paxinos, C. Watson, The Rat Brain in Stereotaxic Coordinates, 2nd ed., Academic Press, San Diego, 1986.
[31] D.E. Pellegrini-Giampietro, J.A. Gorter, M.V. Bennett, R.S. Zukin, The GluR2 (GluR-B) hypothesis: Ca^{2+}-permeable AMPA receptors in neurological disorders, Trends Neurosci. 20 (1997) 464–470.
[32] R.S. Petralia, R.J. Wenthold, Light and electron immunocytochemical localization of AMPA-selective glutamate receptors in rat brain, J. Comp. Neurol. 318 (1992) 329–354.
[33] R.S. Petralia, Y.-X. Wang, E. Mayat, R.J. Wenthold, Glutamate receptor 2-selective antibody shows a differential distribution of calcium-impermeable AMPA receptors among populations of neurons, J. Comp. Neurol. 385 (1997) 456–476.
[34] V. Reja, A.K. Goodchild, J.K. Phillips, P.M. Pilowsky, Tyrosine hydroxylase gene expression in ventrolateral medulla oblongata of WKY and SHR: a quantitative real-time polymerase chain reaction study, Auton. Neurosci.: Basic Clin. 98 (2002) 79–84.
[35] S. Saha, T.F.C. Batten, P.N. McWilliam, Glutamate-immunoreactivity in identified vagal afferent terminals of the cat: a study combining horseradish peroxidase tracing and postembedding electron microscopic immunogold staining, Exp. Physiol. 80 (1995) 193–202.
[36] S. Saha, W. Sieghart, J.-M. Fritschy, P.N. McWilliam, T.F.C. Batten, γ-Aminobutyric acid ($GABA_A$) receptor subunits in rat nucleus tractus solitarii (NTS) revealed by polymerase chain reaction (PCR) and immunohistochemistry, Mol. Cell. Neurosci. 17 (2001) 241–257.
[37] S. Santagati, M. Garnier, P. Carla, E. Violani, G.B. Picotti, A. Maggi, Quantitation of low abundance mRNAs in glial cells using different polymerase chain reaction (PCR)-based methods, Brain Res. Protoc. 1 (1997) 217–223.
[38] K. Sato, H. Kiyama, M. Tohyama, The differential expression patterns of messenger RNAs encoding non-*N*-methyl-D-aspartate glutamate receptor subunits (GluR1–4) in the rat brain, Neuroscience 52 (1993) 515–539.
[39] J.L. Seagard, C. Dean, F.A. Hopp, Properties of NTS neurons receiving input from barosensitive receptors, Ann. N.Y. Acad. Sci. 940 (2001) 142–156.
[40] C.A. Shonis, T.G. Waldrop, Augmented neuronal activity in the hypothalamus of spontaneously hypertensive rats, Brain Res. Bull. 30 (1993) 45–52.
[41] N. Singewald, D. Kouvelas, A. Mostafa, C. Sinner, A. Philippu, Release of glutamate and GABA in the amygdala of conscious rats by acute stress and baroreceptor activation differences between SH and WKY rats, Brain Res. 864 (2000) 138–141.
[42] J.K. Smith, K.W. Barron, Cardiovascular effects of L-glutamate and tetrodotoxin microinjected into the rostral and caudal ventrolateral medulla in normotensive and spontaneously hypertensive rats, Brain Res. 506 (1990) 1–8.
[43] B. Sommer, P.H. Seeburg, Glutamate receptor channels: novel properties and new clones, Trends Pharmacol. Sci. 13 (1992) 291–296.
[44] B. Sommer, K. Keinanen, T.A. Verdoorn, W. Wisden, N. Burnashev, A. Herb, M. Kohler, T. Tagaki, Flip and flop: a cell-specific functional switch in glutamate-operated channels of the CNS, Science 249 (1990) 1580–1584.
[45] K.M. Spyer, Central nervous mechanisms contributing to cardiovascular control, J. Physiol. 474 (1994) 1–19.
[46] T. Suzuki, P.J. Higgins, D.R. Crawford, Control selection for RNA quantitation, BioTechniques 29 (2000) 332–337.
[47] R.M. Sykes, K.M. Spyer, P.N. Izzo, Demonstration of glutamate immunoreactivity in vagal sensory afferents in the nucleus tractus solitarius of the rat, Brain Res. 762 (1997) 1–11.
[48] K. Takayama, M. Miura, Difference in distribution of glutamate-immunoreactive neurons projecting into the subretrofacial nucleus in the rostral ventrolateral medulla of SH and WKY: a double-labeling study, Brain Res. 570 (1992) 259–266.
[49] W.T. Talman, Glutamatergic transmission in the nucleus tractus soli-

tarii: from server to peripherals in the cardiovascular information superhighway, Braz. J. Med. Biol. Res. 30 (1997) 1–7.
[50] W.T. Talman, S.J. Lewis, Altered cardiovascular responses to glutamate and acetylcholine microinjected into the nucleus tractus solitarii of the SH, Clin. Exp. Hypertens., Part A Theory Pract. 13 (1991) 661–668.
[51] W.T. Talman, M.H. Perrone, D.J. Reis, Evidence for L-glutamate as the neurotransmitter of baroreceptor afferent nerve fibers, Science 209 (1980) 813–814.
[52] A. Vardhan, A. Kachroo, H.N. Sapru, Excitatory amino acid receptors in the nucleus tractus solitarius mediate the responses to the stimulation of cardio-pulmonary vagal afferent C fiber endings, Brain Res. 618 (1980) 23–31.
[53] A.J. Verberne, N.A. Young, W.J. Louis, Impairment of inhibitory cardiopulmonary vagal reflexes in spontaneously hypertensive rats, J. Auton. Nerv. Syst. 23 (1988) 63–68.
[54] R.J. Wenthold, N. Yokotani, K. Doi, K. Wada, Immunochemical characterization of the non-NMDA glutamate receptor using subunit-specific antibodies, J. Biol. Chem. 267 (1992) 501–507.
[55] T.L. Yang, C.Y. Chai, C.T. Yen, Enhanced sympathetic reactivity to glutamate stimulation in medulla oblongata of spontaneously hypertensive rats, Am. J. Physiol. 268 (1995) H1499–H1509.
[56] J.C. Yen, J.Y. Chan, S.H. Chan, Differential roles of NMDA and non-NMDA receptors in synaptic responses of neurons in nucleus tractus solitarii of the rat, J. Neurophysiol. 81 (1999) 3034–3043.